Available online at www.sciencedirect.com
SCIENCE DIRECT
Journal of Power Sources 156 (2006) 480–488
JOURNAL OF POWER SOURCES
www.elsevier.com/locate/jpowsour

Hydrogen and dry ice production through phase equilibrium separation and methane reforming☆

Alberto Posada, Vasilios Manousiouthakis*

Chemical Engineering Department, University of California, Los Angeles, CA 90095-1592, USA

Received 8 February 2005; received in revised form 5 April 2005; accepted 5 April 2005
Available online 2 August 2005

Abstract

A clean hydrogen (99.9999%) and dry ice production process is proposed, which is based on phase equilibrium (PE) separation and methane reforming. Heat and power integration studies are carried out for the proposed process, by formulating and solving the minimum hot/cold/electric utility cost problem for the associated heat exchange network. The optimum operating cost of the proposed process is shown to be lower than the corresponding cost of the conventional PSA (pressure swing adsorption) based process, if the produced dry ice is sold for as low as 2 cents kg-dry-ice^{-1} or if an equivalent CO_2 sequestration credit is conceded.

Keywords: Hydrogen; Methane reforming; Dry ice; Heat integration; Power integration; CO_2 sequestration

1. Introduction

The highly efficient oxidation of hydrogen to water in fuel cells suggests it as an environmentally attractive transportation fuel, whose use could result in a positive health impact on city populations [1]. The most common industrial process for production of hydrogen from natural gas is steam reforming [2–4], which involves the endothermic transformation of methane and water to hydrogen, carbon dioxide and carbon monoxide. Following its formation, hydrogen must be separated from the other gases, to attain purity levels required for best performance and long operation of fuel cells [5]. This is especially the case for proton exchange membrane fuel cells (PEMFC), whose anode platinum catalyst has an extremely low carbon monoxide (CO) tolerance (only few ppm) [6]. Hydrogen concentration is increased prior to separation, through the use of water gas shift reactors where CO is partially consumed down to a low percentage as it reacts with water to produce more H_2 and CO_2. Most of the remaining water is later separated by condensation. CO content can sometimes be reduced to few ppm either by using methanation [7] reactors, i.e. catalyzing the reaction of CO with H_2 to produce CH_4, or through CO preferential oxidation (PROX) [8] reactors, which require the addition of precisely measured amounts of air.

Conventional hydrogen production processes, however, [4,9–12] use pressure swing adsorption (PSA) technology for final hydrogen purification [13,14]. PSA achieves separation of CO, CO_2, CH_4 and H_2O from H_2, by adsorption of these components on a solid adsorbent at a relatively high pressure. The adsorbed species are then desorbed from the solid, by lowering the pressure and purging with high purity product hydrogen. The resulting PSA waste gas contains significant amounts of hydrogen and methane and is thus burned as a source of heat for the reformer. Continuous flow of hydrogen product is maintained by using multiple adsorption beds, whose adsorption/desorption cycles are properly synchronized.

In this work, a clean hydrogen (99.9999%) and dry ice production process is proposed, which is based on phase equilibrium (PE) separation and methane reforming. The pro-

☆ Part of this work was first presented in Session 25 at the AIChE 2004 Annual Meeting.

* Corresponding author. Tel.: +1 310 206 0300; fax: +1 310 206 4107.
E-mail address: vasilios@ucla.edu (V. Manousiouthakis).

0378-7753/$ – see front matter © 2005 Elsevier B.V. All rights reserved.
doi:10.1016/j.jpowsour.2005.04.040

Nomenclature

$c_{\mathrm{CUC}j}$	cost coefficient of cold utility with constant temperature number $j = 1, 2, 3$ ($\$\,\mathrm{kJ}^{-1}$)
$c_{\mathrm{CUV}j}$	cost coefficient of cold utility with varying temperature number $j = 1, 2$ ($\$\,\mathrm{kg}^{-1}$)
c_{HU}	cost coefficient of hot utility ($\$\,\mathrm{kg}^{-1}$)
c_{p}	mass heat capacity ($\mathrm{kJ\,kg}^{-1}\,\mathrm{K}^{-1}$)
c_W	cost coefficient of electric utility ($\$\,\mathrm{kJ}^{-1}$)
C	dry ice selling price or CO_2 sequestration credit ($\$\,\mathrm{kg\text{-}dry\text{-}ice}^{-1}$)
CUCj	cold utility with constant temperature number $j = 1, 2, 3$
CUVj	cold utility with varying temperature number $j = 1, 2$
Den	denominator in reaction rate expressions
F	mass flow ($\mathrm{kg\,s}^{-1}$)
HE	heat exchanger subnetwork
HEP	heat engine and pump subnetwork
HU	hot utility
ΔH	enthalpy change ($\mathrm{kJ\,s}^{-1}$)
ΔH°_m	standard (25 °C, 1 atm) heat of reaction r_m, $m = 1, 2, 3$ ($\mathrm{kJ\,mol}^{-1}$)
k_k	adsorption constant of species $k = CH_4$, H_2O, H_2, CO. Units are specified in Table A.1
k_m	rate coefficient of reaction r_m, $m = 1, 2, 3$. Units are specified in Table A.1
K_m	equilibrium constant of reaction r_m, $m = 1, 2, 3$. Units are specified in Table A.2
MUC	minimum utility cost
P_k	partial pressure of species $k = CH_4$, H_2O, H_2, CO_2, CO (bar)
PE	phase equilibrium, PE based process
PSA	pressure swing adsorption, PSA based process
Q	heat flow (negative for cooling) ($\mathrm{kJ\,s}^{-1}$)
ΔS	entropy change ($\mathrm{kJ\,K}^{-1}\,\mathrm{s}^{-1}$)
r_m	reaction $m = 1, 2, 3$
r_{r_m}	rate of reaction r_m, $m = 1, 2, 3$ ($\mathrm{kmol\,kg_{cat}}^{-1}\,\mathrm{h}^{-1}$)
SMR	steam methane reformer
T	temperature (K)
T_i^{H}	high temperature of interval i in the hot temperature scale (K)
T_{i+1}^{H}	low temperature of interval i in the hot temperature scale (K)
$\Delta T_{\min}$	minimum approach temperature (K)
W	electricity (negative if produced) or work (negative if work is done by the fluid) ($\mathrm{kJ\,s}^{-1}$)
W_{s}	work provided to the HEP subnetwork (negative if work is produced) ($\mathrm{kJ\,s}^{-1}$)

Greek letters

α_i	variable indicative of presence of hot utility in interval i
γ_{ji}	variable indicative of presence of cold utility with varying temperature number j in interval i, $j = 1, 2$
δ_i	available heat at interval i ($\mathrm{kJ\,s}^{-1}$)
$\delta_{\mathrm{CUC}j}$	heat transferred to cold utility CUCj ($\mathrm{kJ\,s}^{-1}$)
η_i	fraction of cold composite stream from interval i used in the HE subnetwork
θ_i	fraction of hot composite stream from interval i used in the HE subnetwork
λ_{ji}	variable indicative of presence of cold utility with constant temperature number j in interval i, $j = 1, 2, 3$

Subscripts

C	cold composite stream
cat	catalyst
CUCj	cold utility with constant temperature number $j = 1, 2, 3$
CUVj	cold utility with varying temperature number $j = 1, 2$
H	hot composite stream
HU	hot utility
i	interval i for optimization problem
in	inlet temperature
j	utility number for optimization problem
n	number of intervals for optimization problem
out	outlet temperature
W	electric utility

Superscripts

C	cold temperature scale
CUCj	cold utility with constant temperature number $j = 1, 2, 3$
CUVj	cold utility with varying temperature number $j = 1, 2$
H	hot temperature scale
HU	hot utility

posed flow diagram avoids the following limitations of the PSA based process: (1) close to 12% [12] of the hydrogen produced in the reformer and the water gas shift reactors ends up in the PSA waste gas. (2) A considerable percentage of the methane fed into the reformer is not converted to hydrogen resulting in increased flows through all reaction and separation units; such percentage depends on the reformer operating conditions and it is around 20% [12] for pressure of 25.7 atm, outlet temperature of 1130 K and steam/CH_4 molar ratio of 3.12 in the feed. (3) The unsteady operation of the adsorption (PSA) beds necessitates the use of precise and complex control systems to ensure continuous flow of clean hydrogen. In addition, heat and power integration studies of the proposed PE based process are carried out, with the purpose

of finding the minimum hot/cold/electric utility cost. Use of the same methodology previously applied to the conventional PSA based process [12], allows comparison of operating cost and CO_2 emissions for both processes and leads to our final conclusions.

2. Process description

The proposed hydrogen and dry ice production process, based on phase equilibrium (PE) separation and methane reforming, can be represented with the block diagram in Fig. 1. Water and methane at ambient conditions are fed into this process and transformed into clean hydrogen (99.9999%) and dry ice (98.5%). Chemical transformations only take place in the steam methane reformer (SMR) and are represented by the reversible reactions below:

$$CH_4 + H_2O = CO + 3H_2 \qquad \Delta H_1^\circ : 206.1\,\text{kJ mol}^{-1} \quad (r_1)$$

$$CO + H_2O = CO_2 + H_2 \qquad \Delta H_2^\circ : -41.15\,\text{kJ mol}^{-1} \quad (r_2)$$

$$CH_4 + 2H_2O = CO_2 + 4H_2 \qquad \Delta H_3^\circ : 164.9\,\text{kJ mol}^{-1} \quad (r_3)$$

The kinetics of these reactions on a $Ni/MgAl_2O_4$ catalyst have been studied by Xu and Froment [15] and are listed in Appendix A. Addition of reactions r_1 and r_2 results in reaction r_3, which is the overall steam methane reforming reaction, and thus the overall reactor operation requires that heat be provided to the reformer. Hydrogen is obtained together with all the other species and a purification process is therefore required. A series of phase equilibrium based separation units are used here to sequentially separate H_2O, CO_2, CH_4 and CO, and to obtain a clean hydrogen gas stream. Water is first separated by condensation as the gas stream that exits the reformer is cooled down to almost ambient temperatures. Further cooling to 163 K allows for separation of CO_2 and generation of dry ice. Most of the methane is removed in the CH_4 removal unit A at 77 K and recycled into the reformer, after appropriate heat exchange. CO is absorbed in clean liquid methane [16] (process raw material) that is fed at 86 K into an absorption tower in the CO removal unit. Coming out of this unit, in gas phase at 170 K, methane and the recovered CO are sent to the reformer. CH_4 and CO traces remaining in the hydrogen-rich stream are removed by condensation at 45 K and finally clean gas hydrogen with 99.9999% molar concentration is obtained. Heat exchange and compression operations are used to deliver hydrogen at ambient temperature and 300 atm, which is the typical storage pressure for hydrogen powered vehicles and related hydrogen-fueling stations.

Different than the conventional methane reforming based hydrogen production process [4,9–12], our proposed flow diagram does not use a PSA system for hydrogen purification and does not possess any of the conventional process' limitations described in the previous section.

Water gas shift reactors, typically used to increase hydrogen concentration and reduce CO content of the gas obtained from the reformer, were not considered here since our only purpose is to demonstrate the feasibility of the proposed hydrogen purification process for a flowsheet that only contains a single methane-reforming unit. Nevertheless, similar gas shift reactor containing flowsheets can be developed and will be the subject of future research.

3. Process simulation

The proposed process has been simulated using AspenTech's process engineering software HYSYS® version 3.1 [17]. Peng Robinson's equation of state was used as the thermodynamic fluid package for this simulation, based on AspenTech's recommendation of this package for high hydrogen content systems and after ensuring that the process conditions are within the package's temperature and pressure applicability ranges [18].

The HYSYS process flow diagram is presented in Figs. 1 and 2. The reformer feed is set to 25.7 atm and 811 K, corresponding to values within typical entrance conditions for the reformer [9–11,19–21], and has a steam/CH_4

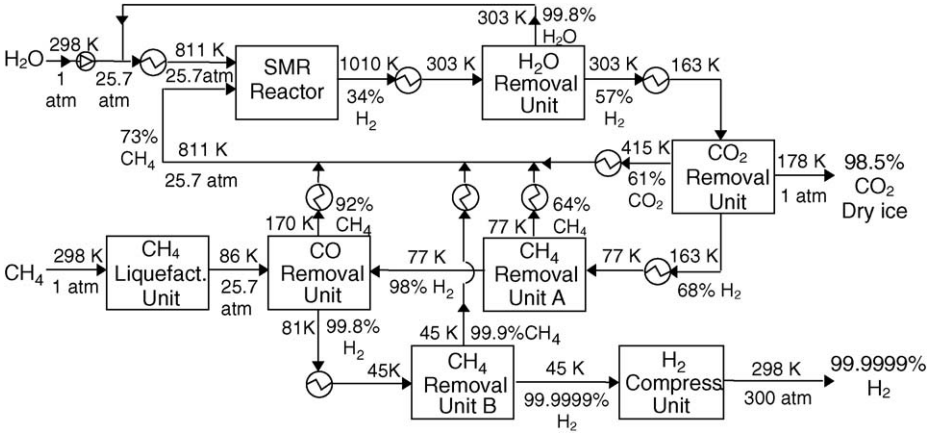

Fig. 1. Process flow diagram for steam methane reforming based hydrogen production with phase equilibrium (PE) based separation. HYSYS simulation.

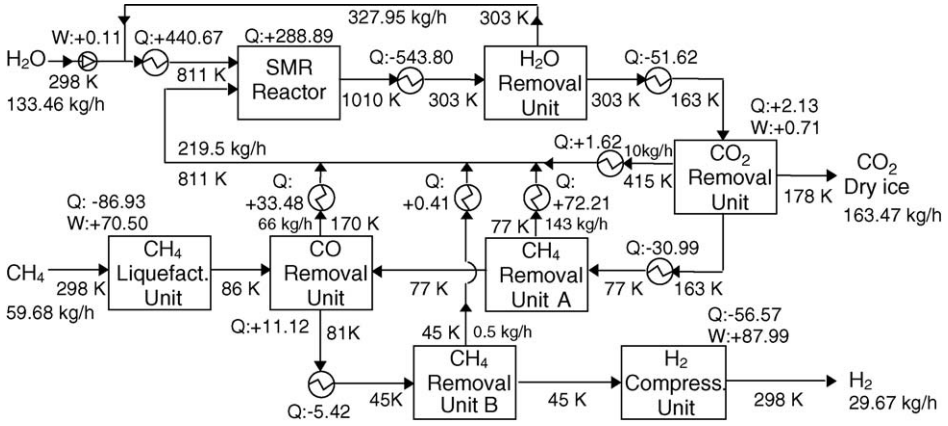

Fig. 2. Process flow diagram for mass and energy flows of the phase equilibrium (PE) based hydrogen plant simulated in HYSYS. Heat (Q) flows are shown as positive (+) for heating and (−) for cooling. Work (W) done on the fluid is shown as (+). Units of energy are kJ s^{-1}.

molar ratio of 3.12. Excess steam is used to reduce by-product carbon formation [4,11,19]. The reformer is simulated using the kinetic models proposed by Xu and Froment [15] (see Appendix A). Heat, in the amount of 288.89 kJ s^{-1}, is provided to the reformer to maintain a high reaction rate. The reformer is modeled in HYSYS® through a series of CSTRs (continuous stirred tank reactors): twenty 2.36-kg_{cat} reactors were considered in this study, with increasing operation temperatures that vary from 825 to 1010 K. The exit mole fraction of hydrogen is calculated to be 0.34.

Hydrogen purification starts with the condensation and flash separation of liquid water from the reformer exit, by cooling the gases to almost ambient temperature through the removal of 543.8 kJ s^{-1}. The condensed water is recycled to the reformer, while the hydrogen containing gas is further cooled to 163 K (through removal of 51.62 kJ s^{-1}) allowing for separation of CO_2 and generation of 163.47 kg h^{-1} of dry ice (98.5% CO_2). The resulting hydrogen-rich gaseous stream is then further cooled to 77 K (through removal of 30.99 kJ s^{-1}) where it is flash separated into a gaseous stream with 98% H_2 and a liquid stream with 64% methane. The last one is recycled into the reformer after addition of 72.21 kJ s^{-1} of heat.

Liquid methane in the amount of 59.68 kg h^{-1} is generated in a liquefaction unit that requires 70.50 kJ s^{-1} of compression work. CO is absorbed in the liquid methane in a 10-equilibrium stage absorption tower used in the CO removal unit, reducing CO content of the hydrogen-rich gas stream to 1 ppm. Net heat of 11.12 kJ s^{-1} is used in the CO removal unit for regeneration of the liquid methane absorbent. Final cooling of 5.42 kJ s^{-1} reduces the temperature of the gas to 45 K, low enough to further remove CH_4 and CO by condensation and obtain 29.67 kg h^{-1} of gas hydrogen with 99.9999% molar concentration (0.37 ppm of CH_4 and 0.12 ppm of CO). The clean hydrogen is then warmed up to ambient temperature, acting as a cold stream for heat integration, and pressurized to 300 atm with the consumption of 87.99 kJ s^{-1} of compression work, considering 85% adiabatic efficiency compressors.

4. Heat and power integration

The approach proposed by Holiastos and Manousiouthakis [22] for the calculation of the minimum hot/cold/electric utility cost for heat exchange networks is employed for the heat/power integration of the above hydrogen/dry ice production process. The problem statement is [22]: given a set of process streams with specified flow rates, inlet temperatures, and fixed outlet target temperatures; hot and cold utility streams with known temperatures and unit costs; and electrical (work) utility with known unit cost; identify, among all possible heat exchange/pump/engine networks, the minimum total (hot/cold/electric) utility cost necessary to accomplish the desired thermal tasks.

For the application at hand, the set of process streams is defined by the material streams in the process flow diagram of Fig. 2; the specifications of the available hot, cold and electric utilities are defined in Table 1. Methane combustion gas is considered as the hot utility available, whose inlet temperature, $T_{in}^{HU} = 2168$ K, is calculated as its adiabatic flame temperature for 110% combustion air and outlet temperature, $T_{out}^{HU} = 313$ K, is estimated for emission. Cooling water with inlet temperature $T_{in}^{CUV1} = 298$ K is the cold utility, which is allowed a 10° increase prior to emission, following heat exchange. The same magnitude of temperature change is considered for cold water with inlet temperature $T_{in}^{CUV2} = 278$ K. Cold utilities with constant temperature are available at $T^{CUC1} = 253$, $T^{CUC2} = 223$ K, $T^{CUC3} = 77$ K (liquid nitrogen). The formulated problem therefore includes both utilities with constant temperature, as Holiastos and Manousiouthakis' [22] formulation does, and utilities with varying temperature, similar to Posada and Manousiouthakis' [12] formulation. The heat and power integration formulation for the case where hot and cold utilities are not allowed to be

Table 1
Utilities specification

Utility[a]	T_{in} (K)	T_{out} (K)	$c_{p\text{-}avg}$[b] (kJ kg^{-1} K^{-1})	Cost ($ kg^{-1})	Cost ($ kJ^{-1})
HU: CH_4 combustion gas	$T_{in}^{HU} = 2168$	$T_{out}^{HU} = 313$	$c_{pHU} = 1.44$	$c_{HU} = 1.724 \times 10^{-2}$[c]	6.45×10^{-6}
CUV1: cooling water	$T_{in}^{CUV1} = 298$	$T_{out}^{CUV1} = 308$	$c_{pCUV1} = 4.31$	$c_{CUV1} = 8 \times 10^{-5}$ [27]	1.85×10^{-6}
CUV2: cold water	$T_{in}^{CUV2} = 278$	$T_{out}^{CUV2} = 288$	$c_{pCUV2} = 4.32$	$c_{CUV2} = 8.6 \times 10^{-4}$ [27]	2×10^{-5}
CUC1	$T^{CUC1} = 253$	$T^{CUC1} = 253$	–	–	$c_{CUC1} = 3.2 \times 10^{-5}$ [27]
CUC2	$T^{CUC2} = 223$	$T^{CUC2} = 223$	–	–	$c_{CUC2} = 6 \times 10^{-5}$ [27]
CUC3: liquid nitrogen	$T^{CUC3} = 77$	$T^{CUC3} = 77$	–	–	$c_{CUC3} = 1.5 \times 10^{-4}$[d]
W: electricity	–	–	–	–	$c_W = 1.25 \times 10^{-5}$ [28]

[a] HU, hot utility; CUV, cold utility with varying temperature; CUC, cold utility with constant temperature; W, electric utility or work.
[b] Average mass heat capacity.
[c] Calculated from cost of 0.3422 $ kg^{-1} for CH_4. Cost of CH_4 is estimated to be energetically equivalent to cost of natural gas (0.3299 $ kg^{-1} [28]).
[d] Calculated as cost of electricity required to liquefy the nitrogen for recycle when using the Stirling gas liquifiers (SLG-1 or SLG-4) from Stirling Cryogenics & Refrigeration BV [29].

used for work generation is given below:

$$\min_{\eta_i,\theta_i,\delta_i,F_{HU},F_{CUV\,j},\delta_{CUC\,j}} \left\{ c_{HU} F_{HU} + \sum_{j=1}^{2} c_{CUV\,j} F_{CUV\,j} + \sum_{j=1}^{3} c_{CUC\,j} \delta_{CUC\,j} + c_W \left(\sum_{i=1}^{n} (Fc_p)_{C,i} (T_i^C - T_{i+1}^C)(1-\theta_i) - \sum_{i=1}^{n} (Fc_p)_{H,i} (T_i^H - T_{i+1}^H)(1-\eta_i) \right) \right\} \quad (1)$$

subject to:

$$\delta_i + [(Fc_p)_{H,i}\eta_i + F_{HU} c_{p_{HU}} \alpha_i](T_i^H - T_{i+1}^H) - \delta_{i+1} - \sum_{j=1}^{3} \delta_{CUC\,j} \lambda_{ji} - \left[(Fc_p)_{C,i}\theta_i + \sum_{j=1}^{2} F_{CUV\,j} c_{p_{CUV\,j}} \gamma_{ji} \right] \times (T_i^C - T_{i+1}^C) = 0 \qquad \forall i \in [1,n] \quad (2)$$

$$\sum_{i=1}^{n} (Fc_p)_{H,i}(1-\eta_i) \ln\left(\frac{T_i^H}{T_{i+1}^H}\right) - \sum_{i=1}^{n} (Fc_p)_{C,i}(1-\theta_i) \ln\left(\frac{T_i^C}{T_{i+1}^C}\right) = 0 \quad (3)$$

$$\delta_i \geq 0 \qquad \forall i \in [2,n] \quad (4)$$

$$\delta_1 = \delta_{n+1} = 0 \quad (5)$$

$$0 \leq \eta_i \leq 1 \qquad \forall i \in [1,n] \quad (6)$$

$$0 \leq \theta_i \leq 1 \qquad \forall i \in [1,n] \quad (7)$$

$$\alpha_i = \begin{cases} 0 & \text{if} \quad T_i^H \leq T_{out}^{HU} \\ 1 & \text{if} \quad T_i^H \leq T_{out}^{HU} \end{cases} \qquad \forall i \in [1,n] \quad (8)$$

$$\gamma_{ji} = \begin{cases} 0 \text{ if} & T_{i+1}^C \geq T_{out}^{CUV\,j} \quad \text{or} \quad T_i^C \leq T_{in}^{CUV\,j} \\ 1 \text{ if} & T_{i+1}^C < T_{out}^{CUV\,j} \quad \text{and} \quad T_i^C > T_{in}^{CUV\,j} \end{cases} \quad \forall i \in [1,n], \forall j = 1,2 \quad (9)$$

$$\lambda_{ji} = \begin{cases} 0 \text{ if} & T_{i+1}^C \neq T^{CUC\,j} \\ 1 \text{ if} & T_{i+1}^C = T^{CUC\,j} \end{cases} \qquad \forall i \in [1,n], \forall j = 1,2,3 \quad (10)$$

$$F_{HU}, F_{CUV1}, F_{CUV2}, \delta_{CUC1}, \delta_{CUC2}, \delta_{CUC3} \geq 0 \quad (11)$$

Nomenclature is provided in a separate section of the paper. The objective function (1), the utility cost, is the sum of the costs of hot, cold and electric utilities. Eq. (2) represents the energy balance in the HE (heat exchanger) subnetwork for each temperature interval. The HE subnetwork is built with heat exchangers; fractions η_i and θ_i of the enthalpies from the hot and cold composite curves in interval i, respectively, are used in this subnetwork. The respective complementary fractions $(1-\eta_i)$ and $(1-\theta_i)$ are used in the HEP (heat engine and pump) subnetwork, built with reversible heat engines and heat pumps. Eq. (3) is the overall entropy balance for the HEP subnetwork. The second law of thermodynamics is expressed in the HE subnetwork by the fact that the available heat at each interval, δ_i, should be non-negative (Eq. (4)). The overall enthalpy balance in the HE subnetwork is ensured by constraint 5. Solution to the formulated problem provides results for heat and power integration of the process. Heat integration only (no power) or pinch analysis [23] can be done by considering only the HE subnetwork, i.e. by setting $\eta_i = 1$ and $\theta_i = 1$ in constraints 6 and 7, respectively.

Table 2
Heat and power integration results

Utility	Conven. process PSA[a] [12]	Heat integ. PSA [12]	Heat and power PSA [12]	Heat integ. PE[b]	Heat and power PE
HU (kJ gH_2^{-1})	10.7	0	0	57.8	1.0
CUV1 (kJ gH_2^{-1})	22.3	24.2	15.1	42.4	14.0
CUV2 (kJ gH_2^{-1})	0	0	0	2.9	0
CUC1 (kJ gH_2^{-1})	0	0	0	0.4	0
CUC2 (kJ gH_2^{-1})	0	0	0	0.8	0
CUC3 (kJ gH_2^{-1})	0	0	0	2.2	0
W[c] (kJ gH_2^{-1})	6.2	6.2	−3.0	19.3	41.4
MUC ($ kgH_2^{-1}) min. utility cost	0.19	0.12	−0.01	1.14	0.55

[a] PSA, pressure swing adsorption based process.
[b] PE, phase equilibrium based process.
[c] W, work or electricity consumed (negative if produced).

5. Results and discussion

The optimization problem is solved using the linear programming software MINOS 5.5 [24]. The calculated minimum utility cost (MUC), expressed per kg of hydrogen produced, is included in the bottom row of the last two columns of Table 2, where complete results are summarized. The first three columns of Table 2, included for comparison, correspond to the results from our previous study [12] on the conventional methane reforming based hydrogen production process with PSA based purification. Specifically, the values in the first column of Table 2 correspond to the conventional PSA based process without any integration analysis (no optimization). The second column corresponds to the results after heat (no power) integration of the PSA based process and the third column corresponds to the results after heat and power integration of the same process. The fourth column contains the results for the heat (no power) integrated PE based process and the fifth column includes the results for the heat and power integrated PE based process.

The enthalpy diagram of the optimal HE network of the PE based process after heat integration is presented in Fig. 3. The solid line corresponds to the hot composite curve and the dotted line represents the cold composite curve. The smallest temperature difference that two streams leaving or entering a heat exchanger can have, termed the minimum approach temperature, is $\Delta T_{min} = 10$ K. It is attained at five so-called pinch temperatures: 453, 302, 288, 258 and 227 K. The use of cooling water (CUV1) in the amount of 349.71 kJ s^{-1} represents almost the whole of the enthalpy change of the cold composite curve between 298 and 308 K (it looks approximately horizontal in Fig. 3 due to the scale of the plot). The remaining small enthalpy change between these temperatures represents water and recycle stream heating prior to their entry in the reformer. The other cold utilities represent smaller amounts of energy whose magnitudes are shown in the fourth column of Table 2. Hot utility, in the amount of 476.10 kJ s^{-1} or 57.8 kJ gH_2^{-1}, is required here to provide heat for the reformer, different than the PSA based process (see Table 2) where sufficient [12] heat is obtained after combustion of the PSA waste gas.

The enthalpy diagram of the optimal HE subnetwork of the PE based process after heat and power integration is presented in Fig. 4. This HE subnetwork does not use cold utilities other than cooling water at 298 K (CUV1), and requires only a very small amount of hot utility.

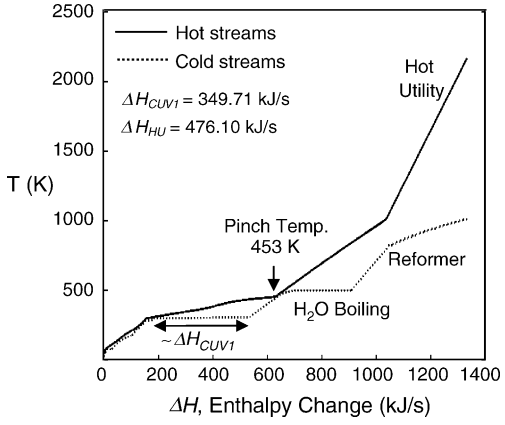

Fig. 3. Enthalpy diagram of the optimal HE network of the methane reforming based hydrogen production process with phase equilibrium (PE) based separation, after heat integration. $\Delta T_{min} = 10$ K.

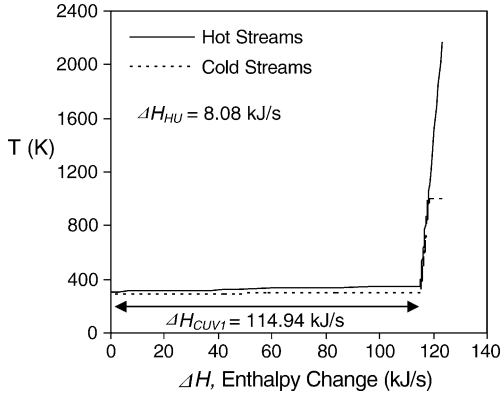

Fig. 4. Enthalpy diagram of the optimal HE subnetwork of the methane reforming based hydrogen production process with phase equilibrium (PE) based separation, after heat and power integration. $\Delta T_{min} = 10$ K.

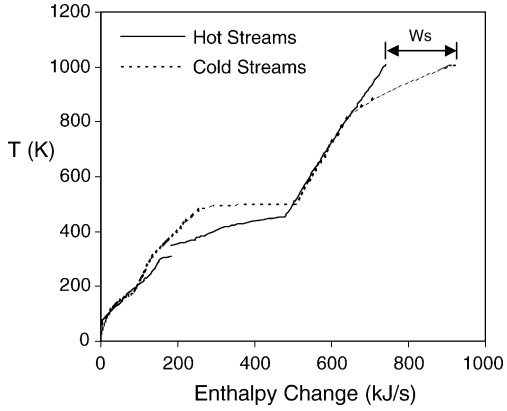

Fig. 5. Enthalpy diagram of the optimal HEP subnetwork of the methane reforming based hydrogen production process with phase equilibrium (PE) based separation, after heat and power integration. $\Delta T_{min,C} = \Delta T_{min,H} = 5$ K. Work required (W_s) is 181.68 kJ s^{-1}.

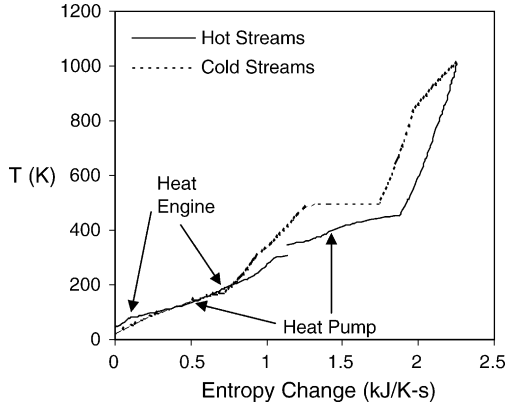

Fig. 6. Entropy diagram of the optimal HEP subnetwork of the methane reforming based hydrogen production process with phase equilibrium (PE) based separation, after heat and power integration. $\Delta T_{min,C} = \Delta T_{min,H} = 5$ K. Entropy changes are balanced: $\Delta S_C = -\Delta S_H$.

The difference in the enthalpy change of the cold composite curve with respect to that of the hot composite curve in Fig. 5 is the net work required by the HEP subnetwork ($W_s = 181.68$ kJ s^{-1}). Addition of this amount to the process work requirements (159.31 kJ s^{-1} or 19.3 kJ gH_2^{-1}) gives the total work needed by the heat and power integrated PE based process (Table 2). The optimal HEP subnetwork is composed of both heat engines and heat pumps, whose corresponding sections can be visualized in the entropy diagram of Fig. 6. Those sections where the hot curve is above the cold require a heat engine, while those where the cold is above the hot require a heat pump. It is easily visualized that a large need for heat pumping exists on the optimal HEP subnetwork.

After comparison of the results shown in Table 2, it is clear that each of the two processes (PSA based and PE based) find their lowest utility cost after heat and power integration and that the PE based process has a much higher utility cost due to its operation at cryogenic temperatures to produce clean hydrogen and dry ice. The economic effects of the production of dry ice (for sale or CO_2 sequestration) and the better use of raw materials attained in the PE based process is taken into account, in addition to the minimum utility cost, with the calculation of the operating cost, as shown in Table 3. The PE based process uses raw materials water and methane in approximately the stoichiometric amounts required by the overall reaction (r_3), which represents reductions of 29% in process methane and 6% in process water with respect to the PSA based process. The operating cost of the PE based process is lowered as a market for the produced dry ice is developed or a CO_2 sequestration credit is conceded. Higher dry ice price/credit (C) obviously results in lower operating cost as shown in Table 3 for values of $C = 16$ and $C = 6$ cents kg-dry-ice^{-1}. It's thus found that if the produced dry ice is sold for as low as 6 cents kg-dry-ice^{-1} or equivalent CO_2 sequestration credit is conceded, the PE based process results in lower operating cost than the heat and power integrated PSA based process. Also shown in Table 3, a value of $C = 2$ cents kg-dry-ice^{-1} results in an operating cost lower than the conventional (without any integration analysis) PSA based process.

Permanent storage of carbon dioxide in the marine environment is described by Murray et al. [25], who propose a technique for the disposal of solid carbon dioxide in the form of dry ice blocks shaped as torpedos that are left to fall through the ocean water to finally penetrate in selected

Table 3
Operating cost

Resource	Conven. process PSA	Heat integ. PSA	Heat and power PSA	Heat integ. PE	Heat and power PE
Process CH_4 (kgCH_4 kgH_2^{-1})	2.84	2.84	2.84	2.01	2.01
Process H_2O (kgH_2O kgH_2^{-1})	4.83	4.83	4.83	4.50	4.50
Dry ice product (kgCO_2 kgH_2^{-1})	0	0	0	5.51	5.51
Operating cost[a] ($ kgH_2^{-1})	1.17	1.10	0.97	$1.83 - C \times 5.51$	$1.24 - C \times 5.51$
If $C = 0.16$[b] ($ kg-dry-ice^{-1})	1.17	1.10	0.97	0.95	0.36
If $C = 0.06$[b] ($ kg-dry-ice^{-1})	1.17	1.10	0.97	1.50	0.91
If $C = 0.02$[b] ($ kg-dry-ice^{-1})	1.17	1.10	0.97	1.72	1.13

[a] Operating cost = MUC + process CH_4 cost + process H_2O cost − dry ice credit. Process water price of 5.3×10^{-4} $ kg^{-1} [27] and methane price of 0.3422 $ kg^{-1} were used.
[b] C: dry ice selling price or CO_2 sequestration credit ($ kg-dry-ice^{-1}).

Table 4
CO_2 emissions

Source	Conven. process PSA	Heat integ. PSA	Heat and power PSA	Heat integ. PE	Heat and power PE
Plant CH_4[a] ($kgCH_4\,kgH_2^{-1}$)	3.05	2.84	2.84	3.10	2.03
Plant CO_2[b] ($kgCO_2\,kgH_2^{-1}$)	8.25	7.71	7.71	2.99	0.05
Work associated CO_2[c] ($kgCO_2\,kgH_2^{-1}$)	0.74	0.74	0	2.31	4.94
Total CO_2[d] ($kgCO_2\,kgH_2^{-1}$)	8.99	8.45	7.71	5.30	4.99

[a] CH_4 consumed in the process (Table 2) or as hot utility (Table 1).
[b] CO_2 emitted from the process or as hot utility. Dry ice not included.
[c] CO_2 emitted (indirectly) as work is generated in a power plant to make it available as a utility. Estimated using a conversion factor for electricity of $0.43\,kgCO_2\,kW^{-1}\,h^{-1}$ [26].
[d] Total CO_2 emission = plant CO_2 + work associated CO_2. Dry ice not included.

deep ocean sediments where the carbon dioxide is chemically sequestered via the formation of a clathrate (CO_2-hydrate) [25].

Calculations of CO_2 emissions are summarized in Table 4. Due to a much lower consumption of CH_4 (for both process and hot utility) and CO_2 sequestration in the form of dry ice, the heat and power integrated PE based process offers a great opportunity for plant CO_2 emission reduction (up to 99%) with respect to the PSA based process, but this brings along the need for additional work that has the potential for an associated CO_2 emission if fossil fuels are used in the generation of such work. Assuming a conversion factor in electricity generation of $0.43\,kg\,CO_2\,kW^{-1}\,h^{-1}$ [26], the total CO_2 reduction is 35% over the heat-power integrated PSA process.

6. Conclusions

A clean hydrogen (99.9999%) and dry ice production process, that employs methane reforming and phase equilibrium (PE) based separation, has been proposed and simulated. Heat and power integration studies have been carried out for the proposed process in order to determine its minimum utility cost. Using this optimum value, the operating cost of this alternative process is then calculated. It is found that if the produced dry ice is sold for as low as 2 cents kg-dry-ice^{-1} or if an equivalent CO_2 sequestration credit is conceded, the PE based process results in lower operating cost than the conventional PSA based process.

After proper disposal of the dry ice, like CO_2 storage in the ocean, the PE based process achieves a 35–99% reduction in CO_2 emissions with respect to the PSA based process, depending on whether or not fossil fuels are used for electricity generation.

Acknowledgement

The authors gratefully acknowledge the financial support of the National Science Foundation under Grant CTS 0301931.

Appendix A. Kinetic models for reactions r_1, r_2 and r_3 in the reformer

Model proposed by Xu and Froment [15] for reactions on a $Ni/MgAl_2O_4$ catalyst:

$$r_{r_1} = \frac{k_1}{Den^2}\left(\frac{P_{CH_4}P_{H_2O}}{P_{H_2}^{2.5}} - \frac{P_{H_2}^{0.5}P_{CO}}{K_1}\right) \tag{A.1}$$

$$r_{r_2} = \frac{k_2}{Den^2}\left(\frac{P_{CO}P_{H_2O}}{P_{H_2}} - \frac{P_{CO_2}}{K_2}\right) \tag{A.2}$$

$$r_{r_3} = \frac{k_3}{Den^2}\left(\frac{P_{CH_4}P_{H_2O}^2}{P_{H_2}^{3.5}} - \frac{P_{H_2}^{0.5}P_{CO_2}}{K_3}\right) \tag{A.3}$$

where

$$Den = 1 + k_{CO}P_{CO} + k_{H_2}P_{H_2} + k_{CH_4}P_{CH_4} + k_{H_2O}\left(\frac{P_{H_2O}}{P_{H_2}}\right) \tag{A.4}$$

The rate coefficients and adsorption constants are given in Table A.1 and the reaction equilibrium constants in Table A.2.

Table A.1
Rate coefficients and adsorption* constants' parameters for related Arrhenius or Van't Hoff* equations

Rate coefficient or adsorption* constant	Pre-exponential factor	Units of pre-exponential factor	Activation energy or adsorption* enthalpy ($kJ\,mol^{-1}$)
k_1	4.225×10^{15}	$kmol\,bar^{0.5}\,kg_{cat}^{-1}\,h^{-1}$	240.1
k_2	1.955×10^{6}	$kmol\,kg_{cat}^{-1}\,h^{-1}\,bar^{-1}$	67.13
k_3	1.020×10^{15}	$kmol\,bar^{0.5}\,kg_{cat}^{-1}\,h^{-1}$	243.9
k_{CO}*	8.23×10^{-5}	bar^{-1}	−70.65*
k_{CH_4}*	6.65×10^{-4}	bar^{-1}	−38.28*
k_{H_2O}*	1.77×10^{5}	dimensionless	88.68*
k_{H_2}*	6.12×10^{-9}	bar^{-1}	−82.90*

Table A.2
Reaction equilibrium constants

Equilibrium constant	Function of T (K)	Units of equilibrium constant
K_1	$\exp(-26{,}830/T + 30.114)$	bar^2
K_2	$\exp(4{,}400/T - 4.036)$	dimensionless
K_3	$K_1 \times K_2$	bar^2

References

[1] National Research Council, The Hydrogen Economy: Opportunities, Cost, Barriers, and R&D Needs, The National Academies Press, Washington, D.C., 2004.
[2] W.H. Scholz, Gas Sep. Purif. 7 (1993) 131–139.
[3] P.L. Spath, M.K. Mann, Life Assessment of Hydrogen Production via Natural Gas Steam Reforming, Technical report NREL/TP-570-27637, National Renewable Energy Laboratory, Golden, CO, 2001.
[4] J.N. Armor, Appl. Catal. A: Gen. 176 (1999) 159–176.
[5] G. Hoogers, Fuel Cell Technology Handbook, CRC Press LLC, Boca Raton, 2003.
[6] G. Hoogers, D. Thompsett, Chem. Ind.-London 20 (1999) 796–800.
[7] S. Takenaka, T. Shimizu, K. Otsuka, Int. J. Hydrogen Energ. 29 (2004) 1065–1073.
[8] Y. Choi, H.G. Stenger, J. Power Sources 129 (2004) 246–254.
[9] S.M. Leiby, Options for Refinery Hydrogen, PEP Report No. 212, Process Economics Program, SRI International, Menlo Park, CA, 1994.
[10] J.R. Hufton, S. Mayorga, S. Sircar, AIChE J. 45 (1999) 248–256.
[11] J.K. Rajesh, S.K. Gupta, G.P. Rangaiah, A.K. Ray, Chem. Eng. Sci. 56 (2001) 999–1010.
[12] A. Posada, V. Manousiouthakis, Heat and Power Integration Opportunities in Methane Reforming based Hydrogen Production with PSA Separation, AIChE 2004 Annual Meeting Conference Proceedings, paper 22f, 2004.
[13] S. Sircar, Ind. Eng. Chem. Res. 41 (2002) 1389–1392.
[14] D.M. Ruthven, S. Farooq, K.S. Knaebel, Pressure Swing Adsorption, Wiley, New York, 1994.
[15] J. Xu, G.F. Froment, AIChE J. 35 (1989) 88–96.
[16] M. Ogawa, T. Seki, H. Honda, M. Nakamura, Y.A. Takatani, Electr. Eng. Jpn. 147 (2004) 32–42.
[17] http://www.aspentech.com/brochures/HYSY.S.pdf, AspenTech.
[18] http://www.massbal.com/support/hysim/sim_hints.asp, AspenTech.
[19] B. Tindall, D. King, Hydrocarb. Process. 73 (1994) 69–75.
[20] G.H. Shahani, L.J. Garodz, K.J. Murphy, W.F. Baade, P. Sharma, Hydrocarb. Process. 77 (1998) 143–149.
[21] J.M. Ogden, Review of Small Stationary Reformers for Hydrogen Production, Center for Energy and Environmental Studies, Princeton University, Princeton, NJ, 2001.
[22] K. Holiastos, V. Manousiouthakis, Comput. Chem. Eng. 26 (2002) 3–16.
[23] B. Linnhoff, Chem. Eng. Res. Des. 71 (1993) 503–522.
[24] http://www.sbsi-sol-optimize.com/manuals/Minos#Manual.pdf, Stanford Business Software Inc.
[25] C.N. Murray, L. Visintini, G. Bidoglio, B. Henry, Energ. Convers. Manage. 37 (1996) 1067–1072.
[26] http://www.defra.gov.uk/environment/envrp/gas/05.htm, UK Department for Environment, Food and Rural Affairs.
[27] M.S. Peters, K.D. Timmerhaus, R.E. West, Plant Design and Economics for Chemical Engineers, fifth ed., McGraw-Hill, New York, 2003, p. 266.
[28] http://www.eia.doe.gov, US Department of Energy.
[29] http://www.stirling.nl/menu.html, Stirling Cryogenics & Refrigeration BV.